Disruption of *Caenorhabditis elegans* Muscle Structure and Function Caused by Mutation of Troponin I

A. K. Burkeen,* S. L. Maday,* K. K. Rybicka,† J. A. Sulcove,* J. Ward,† M. M. Huang,‡ R. Barstead,‡ C. Franzini-Armstrong,† and T. StC. Allen*

*Biology Department, Oberlin College, Oberlin, Ohio; †Pennsylvania Muscle Institute and Department of Cell and Developmental Biology, University of Pennsylvania, Philadelphia, Pennsylvania; and ‡Oklahoma Medical Research Foundation, Program in Molecular Biology, Oklahoma City, Oklahoma

ABSTRACT *Caenorhabditis elegans* strains mutant for the *unc-27* gene show abnormal locomotion and muscle structure. Experiments revealed that *unc-27* is one of four *C. elegans* troponin I genes and that three mutant alleles truncate the protein: recessive and presumed null allele *e155* terminates after nine codons; semidominant *su142*sd eliminates the inhibitory and C-terminal regions; and semidominant *su195*sd abbreviates the extreme C-terminus. Assays of in vivo muscular performance at high and low loads indicated that *su142*sd is most deleterious, with *e155* least and *su195*sd intermediate. Microscopy revealed in mutant muscle a prevalent disorder of dense body positioning and a less well defined sarcomeric structure, with small islands of thin filaments interspersed within the overlap region of A bands and even within the H zone. The mutants' rigid paralysis and sarcomeric disarray are consistent with unregulated contraction of the sarcomeres, in which small portions of each myofibril shorten irregularly and independently of one another, thereby distorting the disposition of filaments. The exacerbated deficits of *su142*sd worms are compatible with involvement in vivo of the N-terminal portion of troponin I in enhancing force production, and the severe impairment associated with *su195*sd highlights importance of the extreme C-terminus in the protein's inhibitory function.

INTRODUCTION

Nearly a century ago, A. V. Hill (1927) drew attention to a problem that remains incompletely solved, namely how muscular performance is varied from one striated muscle to the next despite considerable similarity in structure. One solution likely lies in the rich diversity of muscle protein isoforms. In the case of troponin, which confers calcium sensitivity on the interaction of actin with myosin and hence on tension development, it has been difficult to understand how sequence differences among the isoforms of each of the three subunits might alter calcium regulation and muscular function, given a lack of information concerning the in vivo role of domains of each subunit. Shedding light on these roles, experiments reported here examine with *Caenorhabditis elegans* the functional and structural impairment caused by three truncation mutations of troponin I (TnI), the subunit responsible for inhibiting actin-myosin interaction.

Recent structural analysis of crystalline human cardiac troponin (Takeda et al., 2003) complements extensive biochemical work (comprehensively reviewed by Perry, 1999), and both provide the framework of current understanding of the protein switch. The core of crystalline troponin, bound with calcium, appears to comprise an arm flexibly linked to a regulatory head. The so-called IT-arm is formed from the first two of four α-helices of TnI, the C-terminal half of troponin C (TnC), and a portion of the C-terminal half of troponin T (TnT). The head is built from the third α-helix of TnI and the N-terminal half of TnC. Toggling of the troponin switch from on, as represented by the crystalline structure, to off is envisaged to involve dissociation of TnI's third helix from the N-lobe of TnC and the subsequent association of the C-terminal half of TnI with actin-tropomyosin (Takeda et al., 2003).

Experiments with model genetic organisms expressing troponin mutations allow testing of the proposed function of troponin within intact muscle in vivo, and the extraordinary conservation of muscle composition, organization, and function suggests that such studies can yield information broadly applicable. The nematode *C. elegans* moves through the use of four strips, or quadrants, of obliquely striated muscle (termed body-wall muscle) running the length of the worm and operating in conjunction with a hydrostatic skeleton (*C. elegans* muscle development, organization, and function are comprehensively reviewed by Moerman and Fire, 1997). Body-wall muscle contracts at 0.1–2 Hz during the worm's locomotion, and tension development is regulated by troponin, although some evidence (Harris et al., 1977) exists for myosin-linked regulation or modulation, as well. Among existing *C. elegans* mutants, the *unc-27* class drew our attention, because its phenotype (rigidity, sluggishness, and sarcomeric disorganization; Brenner, 1974; Zengel and Epstein, 1980) suggested defects in the troponin switch. Moreover, the position of *unc-27* on the mutation-based genetic map correlates well with the position of DNA potentially encoding TnI on the clone-based physical map. Allowing a rare opportunity to examine the role of particular TnI domains in vivo, the experiments

Submitted February 21, 2003, and accepted for publication September 24, 2003.

Address reprint requests to Taylor Allen, Biology Department, Oberlin College, 119 Woodland St., Oberlin, OH 44074-1097. Tel.: 440-775-8324; Fax: 440-775-8960; E-mail: taylor.allen@oberlin.edu.

0006-3495/04/02/991/11 $2.00

reported here identify *unc-27* as a TnI gene and examine the functional and structural impairment caused to body-wall muscle by the three available mutant alleles.

METHODS

Nomenclature and maintenance of strains

In addition to the N2 wild-type strain of *C. elegans* variant Bristol, the following alleles of *unc-27*, on chromosome *X*, were used: *su142*sd, *e155*, and *su195*sd. The naming is descriptive. The mutant alleles define the 27th family of mutant worms having uncoordinated movement as the originally described and most easily detected phenotype. The letter prefix in the allele name refers to the laboratory of isolation, and the letter suffix, when present, indicates characteristics of the mutation, *e.g.*, semidominance in the case of *su142*sd and *su195*sd. Strains were handled according to published methods (Brenner, 1974).

Transformation rescue

Cosmid ZK721, which spans a TnI gene predicted to lie in the vicinity of *unc-27* on the genetic map, was injected into a strain carrying the temperature-sensitive genetic marker *pha-1*(*e2123*). The injected DNA included a cloned copy of the wild-type *pha-1* gene to allow selection of transformants. For both of the stably transformed lines recovered, PCR with primers matching sequences unique to ZK721 was used to confirm the presence of ZK721 in the transformed lines. Standard genetic crossing enabled introduction of the transformed copy of the TnI gene into a strain carrying *unc-27*(*e155*). The chromosomal genotype of the resulting strains was *pha-1*(*e2123*)*III; unc-27*(*e155*)*X*. In addition, the resulting strains carried one of the two extrachromosomal elements containing transformed copies of the *pha-1* gene and of ZK721. As assayed by motility and muscle organization, the transformed copies of ZK721 rescued the *unc-27* mutant phenotype. Further, as expected, the *unc-27* mutant phenotype reappeared when the extrachromosomal element was allowed to segregate away.

Analysis of TnI sequences

Four genomic regions potentially encoding TnI were identified by a search with BLAST (Altschul et al., 1990), using default settings, of GenBank (url: www.ncbi.nlm.nih.gov) for sequences similar to rabbit fast twitch TnI. The activity of the four loci as bona fide genes was confirmed by amplification of wild-type cDNA for each, and the exon-intron boundaries of the genes followed from comparison of the genomic sequences deposited in Genbank with cDNA sequences. The cDNA was prepared from total RNA isolated from ~0.1 g N2 worms with Trizol per its accompanying protocol (Invitrogen, Carlsbad, CA), and sequencing was done with the Silver Sequencing Kit (Promega, Madison, WI). Sites of mutation were identified through sequencing of genomic DNA isolated from single mutant worms (Williams et al., 1992) and amplified under conditions promoting high fidelity (either with ~25 μM of each nucleotide or with the proofreading polymerase pfu (Stratagene, La Jolla, CA)) using primers specific to locus ZK721.2. Mutations were verified by sequencing multiple independent genomic DNA clones, as well as ZK721.2 cDNA that had been prepared from mutant strains.

Accession numbers of TnI sequences used to determine the evolutionary relationships among TnI isoforms follow: *C. elegans* F42E11.4 (Z66562), *C. elegans unc-27*/ZK721.2 (U40951), *C. elegans* T20B3.2 (Z81593), *C. elegans* W03F8.1 (AF039041), *Chlamys nipponensis* (Japanese scallop) (JE0233), *Drosophila melanogaster* heldup (P36188), *Astacus astacus* (broad-fingered crayfish) (A31484), *Homo sapiens* cardiac (P19429), *H. sapiens* slow (P19237), *H. sapiens* fast (AJ245761), *Oryctolagus cuniculus* (rabbit) cardiac (P02646), *O. cuniculus* slow (P02645), *O. cuniculus* fast (P02643), *Coturnix coturnix* (quail) cardiac (A41030), *C. coturnix* slow (U37118), *C. coturnix* fast (A23569), and *Salmo salar* (salmon) fast (U83878). Sequences were aligned using ClustalX at default settings (Thompson et al., 1997), followed by minor adjustment by eye to ensure proper alignment of characteristic TnI protein motifs. Phylogenetic analysis to identify evolutionary relationships was performed in PAUP v4.0b8 (Swofford, 2000) using the branch and bound search analysis followed by a full heuristic bootstrap analysis using 1000 replicates. The Gibbs and Motif algorithms (url: www.blocks.fhcrc.edu) were used to define conserved blocks within aligned sequences (Henikoff et al., 1995).

Localization of mRNA

TnI RNA was localized in larvae and adults with digoxigenin-labeled single-stranded DNA probes complementary to 3′UTR by the procedure of Kolmerer et al. (2000). The signal generated in this procedure is a stable, dark precipitate at sites with probes, and the anatomical location of this signal is readily identified via differential interference microscopy. Probes were reacted with embryos in the manner of Greenstein et al. (1994) and detected by the procedure of Kolmerer et al. (2000).

RNA interference

T7 RNA polymerase promoter sites were incorporated at the 5′ end of primers specific to the TnI isoforms, and PCR was used to generate sufficient double-stranded DNA template, purified on agarose gels, for transcription with the AmpliScribe T7 Kit (Epicentre, Madison, WI). The transcription product was denatured and reannealed to ensure a high percentage of double-stranded RNA by heating for 10 min at 75°C and cooling to 37°C over 30 min. Elimination of F42E11.4 transcripts from embryos, by RNA interference (RNAi) with fourth-stage larvae (L4) and recovery of progeny, caused significant embryonic lethality (of 266 progeny produced within 24 h by 6 treated wild-type hermaphrodites, 160 arrested as early embryos). Thus, RNAi was performed by soaking first-stage larvae (L1) for 24 h in solution containing 1–2 μg/μl RNA in the manner of Maeda et al. (2001), and worms were examined ~72 h later, by which time they had attained adulthood.

Electron microscopy

Adult worms were fixed in 3% glutaraldehyde in 0.1 M Na cacodylate buffer, pH 7.2–7.4, on ice for 3 h, cut transversely in half in glutaraldehyde, and left in the fixative at room temperature overnight. Next day, the worms were washed in buffer, postfixed in 2% OsO_4 in cacodylate buffer for 1 h, washed in water and en-block stained in saturated aqueous uranyl acetate for 1 h, all at room temperature. All material was dehydrated in graded concentrations of ethyl alcohol (EtOH; 15 min each in 70% and 90%) followed by three changes each of absolute EtOH and acetone; material was then embedded in Epon. Ultrathin sections were stained with 3% uranyl acetate in 50% EtOH and with lead salts (Sato, 1968), and they were photographed in a Philips 410 EM.

Immunofluorescence and polarized light microscopy

Worms were labeled with mouse antivinculin (MH24, a kind gift of M. Coutu Hresko, Washington University, St. Louis, MO) at a dilution of 1:200 by the procedure described by Finney and Ruvkin (1990), as modified by Miller and Shakes (1995). The fixative contained 2% formaldehyde and 25% v/v methanol. The secondary antibody was goat antimouse conjugated with fluorescein (AP181F, Chemicon International, Temecula, CA). Polarized light microscopy with live worms was achieved by inserting between the ocular and plan apochromat objective a sheet polarizer crossed in orientation with a polarizer between the condenser and light source of an Eclipse TE300 (Nikon,Tokyo, Japan).

Tests of locomotion and measurements of sizes

For dimensional analysis, worms were synchronized in growth and photographed at defined ages via a camera attached to a stereomicroscope (MZFlIII, Leica, Bannockburn, IL). Negatives were digitized, magnified, and printed, allowing measurement of the length and diameter. For swimming assays, worms were transferred from agar plates to liquid (unless specified otherwise in text, solution was 0.1 M NaCl, 50 mM potassium-phosphate, pH 6) and were given 30 s to recover from the transfer before commencement of the measurement, which involved counting the contractile waves propagating along the length of worms during 60 s. The creeping behavior of worms was assessed in the manner of Epstein et al. (1976), who used a chemotaxis assay to resolve differences in crawling capability among strains. *C. elegans* move toward and feed on bacteria. In the assay, a drop of 10–100 age-synchronized adults in a minimal volume of liquid (<2 μl) was placed at the center of a ring of bacteria, and the chemotaxis of worms from the center toward the ring was monitored. Statistical significance was evaluated with Student's *t*-test and the Wilcoxon-Mann-Whitney test for comparison of two populations; for multiple comparisons, ANOVA was used and followed when appropriate with a post hoc test (Tukey's honestly significant difference test and Games-Howell test, both within SPSS version 11.5).

RESULTS

Linkage of *unc-27* with TnI and identification of multiple TnI isoforms

Two lines of evidence showed that the *C. elegans unc-27* gene encodes TnI. First, a transformed wild-type copy of the TnI gene on cosmid ZK721 completely rescued *unc-27* worms from the mutant phenotype (see Materials and Methods). Second, mutations in this TnI gene were found for the three *unc-27* mutant alleles: Gln^{10}stop for *e155*, Gln^{122}stop for *su142*sd, and Glu^{207}stop for *su195*sd. Fig. 1 aligns the inferred amino acid sequence of the TnI encoded by ZK721 with representative vertebrate TnIs, as well as with three other *C. elegans* TnI isoforms uncovered via similarity searches of genetic data deposited in GenBank by the *C. elegans* mapping/sequencing consortium. These other isoforms are F42E11.4 (on the X chromosome), T20B3.2 (on chromosome V), and W03F8.1 (on chromosome IV).

Conservation of sequence among TnIs, although particularly striking over the region termed the inhibitory peptide (underlined in Fig. 1 and corresponding to residues Asn^{96}-Met^{116} of rabbit fast TnI, accession No. P02643, with glycine of the second codon taken as residue 1), can be categorized into several blocks, detected in a search of seventeen invertebrate and vertebrate TnI sequences with the MOTIF and GIBBS algorithms. Referenced to the sequence of rabbit fast TnI, these blocks follow: MOTIF block 1, Lys^{5} to His^{47}; MOTIF block 2, Tyr^{79} to Val^{114}; MOTIF block 3, Lys^{129} to Glu^{151}; Gibbs block 1, Leu^{63} to Val^{114}; and Gibbs block 2, Asp^{135} to Glu^{151}. The similarity of size of N-terminal extensions in vertebrate cardiac and worm TnIs hinted of a stronger evolutionary relationship between these two classes than between vertebrate skeletal and cardiac isoforms, but evolutionary analysis (Fig. 2) did not support this idea. The clustering of chordate troponins by muscle-specific isoform (*e.g.*, cardiac) rather than by species suggests that diversification into multiple isoforms occurred in a common ancestor to these chordates. However, the *C. elegans* isoforms do not cluster with any vertebrate equivalent, indicating that the diversification of invertebrate isoforms occurred independently.

In wild-type worms, ZK721.2/*unc-27* is transcriptionally active in the body-wall musculature, with weak expression in late-stage embryos (Fig. 3 *A*) and strong expression during the larval and adult stages (Fig. 4, *A* and *B*), when it appears to be the major body-wall isoform. Transcripts were also detected in the diagonal sex muscles of the male (Fig. 4 *B*). F42E11.4 is the major body-wall isoform during embryogenesis (Fig. 3 *B*), but its body-wall expression wanes during the larval stages. In late-stage larvae and adults, expression

```
ZK721.1                MSE EAG-EDAQ*RKAAE-- REAKKAEVRKRLEEA GNKKKAKKGFLTPER KKKLRKLLMVKAAED  60
F42E11.4      MSQIDENIRYGGAAN ETDGEDAQRKAQE-- REAKKAEVRKRLEEA GQK-KQKKGFLTPER KKKLRKLLMNKAAED  72
T20B3.2       MLIEDENIRYGGAQA DVE-DDAARKAQE-- RELKKAEVRKRMEEA AKKGSKKKGFLTPER KKKLRKLLMMKAAED  72
W03F8.1                MS DVDADEVSRGAQNGG RERKKEEVRKRLEEA SRMKKAKKGFLTPER KKKLRKLLMMKAAED  62
HumanCardiac           MADG SSDAAREPRPAPAPI RRRSSNYRAYATEPH AKK----KSKISASR KLQLKTLLLQIAKQE  60
RabbitSlow                                              PE VER----KSKITASR K-LLKSLMLAKAKEC  27
RabbitFast                                              GD EEK----RNRAITAR RQHLKSVMLQIAATE  28

ZK721.1       LKRQQLLKEQERQKA LADRTISLPNVDSID DKGQLEKIYNDLWAR LTQLEEEKYDINYVV SQ*TEAEINSLTIEVN 135
F42E11.4      LKTQQLRKEQERVKV LAERTVALPNVDSID DHAKLEAIYNDLFSR LCNLEEEKYDINHIT TETETTINQLNIEVN 147
T20B3.2       LKQQQMLKEQERQKT LQQRTIPLPDVDSIN DQGQLLKIYEDMFAR VCALEEEKFDINFGV SQTEAEINQLTIQVN 147
W03F8.1       LKQQQMLKEQERQRI LQERIIPLPDLDNED D---LEAVYDEIRER LIDLESENYDVSYIV RQKDFEINELTIAVN 134
HumanCardiac  LEREAEERRGEKGRA LSTRCQPLELAGL-- GFAELQDLCRQLHAR VDKVDEERYDIEAKV TKNITEIADLTQKIF 133
RabbitSlow    -QQEHEAREAEKVRY LAERIPALQTRGL-- SLSALQDLCRQLHAK VEVVDEERYDIEAKC LHNTREIKDLKLKVL  99
RabbitFast    LEKEEGRREAEKQNY LAEHCPPLSLPG--- SMAEVQELCKQLHAK IDAAEEEKYDMEIKV QKSSKELEDMNQKLF 100

ZK721.1       DLRGKFVKPSLKKVS KYDNKFKKSGESKAG T-KEDFRANLKIVKK -DVMEAIVNVKKK-- -DDKPDWSKKNKDAK 205
F42E11.4      DLRGKFVKPSLKKVS KYDNKFKKMAEAKKE DGSKNLRNNLKTVKK -ESVFTQIANKKK-- -SDKPEWSKKKEE-K 217
T20B3.2       DLRGKFVKPTLKKVS KYDNKFKSSGEVKE- --KSNFRNNLKVVKK -ETDLDEIMAKKKGT ADGKPEWSKKEK--K 216
W03F8.1       DLRGKFVKPTLKKVS KTEGKFDKLKKKEAT --KVDFRAQLKVVDK NEFALDEEDTEKK-- -E-KAAWAK       197
HumanCardiac  DLRGKFKRPTLRRVR ISADAMMQALLGARA KESLDLRAHLKQVKK ------EDTEKEN-- -REVGDWRKNIDALS 199
RabbitSlow    DLRGKFKRPPLRRVR VSADAMLRALLGSKH KVSMDLRANLKSVKK ------EDTEKER-- PVEVGDWRKNVEAMS 166
RabbitFast    DLRGKFKRPPLRRVR MSADAMLKALLGSKH KVCMDLRANLKQVKK ------EDTEKERDL -RDVGDWRKNIEEKS 168

ZK721.1       A*EDSAP----AAVAP EAEP---VAEEAEAE PEAEEEEGEEEEEE 242
F42E11.4      KEESAP-------EP VIEP---VEEEETAA SEGEEEE-EEADEE 250
T20B3.2       EEEAAPVELAAPVEP EAEPEPEAAEPAAEE PEAEEEEEEEEEEE 260
HumanCardiac  GMEGRK--------K KFES                          210
RabbitSlow    GMEGRK--------K MFDA----AKSPTSQ                184
RabbitFast    GMEGRK--------K MFES----ES                     181
```

FIGURE 1 Alignment of the inferred amino acid sequence of the TnI encoded by ZK721.2/*unc-27* with the three other *C. elegans* isoforms (F42E11.4, T20B3.2, and W03F8.1), as well as with human cardiac TnI (accession No. P19429) and with rabbit slow (accession No. P02645) and fast isoforms (accession No. P02643). Asterisks mark sites of mutation of ZK721.2: Gln^{10}stop for *e155*; Gln^{122}stop for *su142*sd; and Glu^{207}stop for *su195*sd. The region corresponding to the inhibitory peptide (rabbit fast TnI residues Asn^{96}–Met^{116}) is underlined.

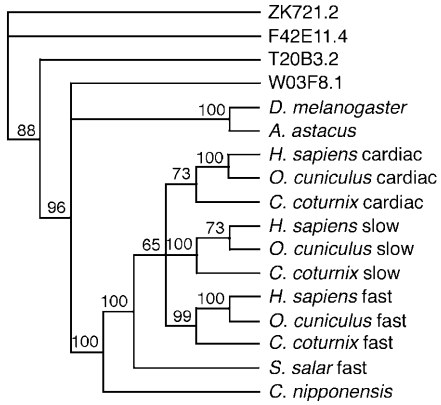

FIGURE 2 A phylogenetic array comparing troponin I isoforms of vertebrates and invertebrates suggests that diversification of troponin I isoforms occurred independently in the two lineages. Bootstrap probabilities are noted at each node.

of F42E11.4 is evident in the proximal gonad of both hermaphrodites (Fig. 4, *C* and *D*) and males (Fig. 4 *E*). T20B3.2 (Figs. 3 *C* and 4, *F* and *G*) transcripts were detected in the body-wall musculature, but expression in hermaphrodites appeared limited to the anteriormost body-wall muscle cells. Expression in the body-wall muscle of males was less restricted, typically including posterior body-wall muscle cells, in addition to those at the head (Fig. 4 *G*). T20B3.2 transcripts were found also in the vulval muscles of hermaphrodites and the sex muscles of males (Fig. 4, *F* and *G*). From embryos to adults, expression of W03F8.1 was detected only in pharyngeal muscle cells (Figs. 3 *D* and 4 *H*).

When compared, the mutants evidenced similar expression patterns that differed in two respects from the wild-type

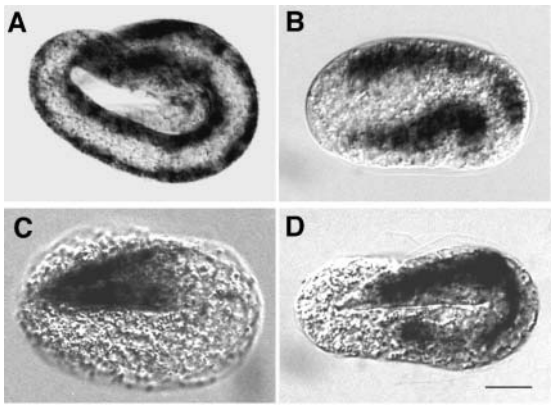

FIGURE 3 Localization of TnI mRNA in embryos. (*A*) ZK721.2/*unc-27* transcripts in body-wall muscle of threefold embryo. (*B*) F42E11.4 in body-wall muscle of 1.25-fold embryo. (*C*) T20B3.2 in anteriormost body-wall muscle cells of threefold embryo. (*D*) W03F8.1 in pharyngeal musculature of threefold embryo. In all panels, embryos are positioned with head pointing to the left. Scale, 10 μm.

patterns: in each of the mutant strains, transcripts of F42E11.4 (Fig. 4 *I*) and T20B3.2 (Fig. 4 *J*) were detected in body-wall muscle of a fraction of adult hermaphrodites (mutant males were not examined; in mutant larvae, expression of T20B3.2 matched that of wild-types). This fraction, for animals showing staining, was ~0.3 for F42E11.4; it was ~0.1 for T20B3.2 with *su142*sd and *e155* worms, but ~0.5 with *su195*sd worms. Expression of body-wall isoforms of TnT (Fig. 4, *K* and *L*) and TnC (Fig. 4 *M*) in the mutants resembled the wild-type patterns (Allen et al., 1997; Terami et al., 1999), with the exception that transcripts of the major embryonic body-wall TnT (*mup-2*/*tnt-1*/T22E5.5) remained detectable in body-wall muscle of some mutant adults.

Extent of paralysis of *unc-27* mutants

The locomotion of mutants was clearly compromised, indicative of deficits in the activation and relaxation of muscle. In the swimming assay, a comparatively low-force/high-velocity test, impairment was apparent as early as the first larval stage and grew worse as the worms developed (Table 1). Additionally, the severity of the mutations (''allelic strength'') differed: adults homozygous for *e155* operated their body-wall muscle in this assay at one-third of the wild-type frequency, whereas mutants homozygous for *su142*sd or for *su195*sd operated at about one-ninth. The somewhat compromised swimming behavior of *su142*sd and *su195*sd heterozygotes, with one wild-type and one mutant copy of *unc-27*, confirms the designation of these mutations as semidominant. Moreover, given the absence of haploinsufficiency (i.e., given that heterozygotes with one wild-type allele and one null allele, *e155*, are indistinguishable from wild-type homozygotes), the semidominance of these mutations offers strong evidence that they are manifested at the protein level. Performance of the mutants in the chemotaxis assay, a comparatively low-velocity/high-force test, also differed from that of wild-types. Fig. 5 displays the results, showing a rapid migration of wild-types to food ($t_{1/2}$ = 3.29 $\pm$ 0.48 min, n =7 trials) and slower movement of mutants ($t_{1/2}$ = 24.35 $\pm$ 4.56 min for *e155*, 25.07 $\pm$ 5.62 min for *su195*sd, and 59.72 $\pm$ 5.17 min for *su142*sd; n = 4 trials with each).

Whether variations in compensation by wild-type TnI (possibly F42E11.4 and T20B3.2, as suggested by the data on expression patterns) for mutant ZK721.2/UNC-27 protein contributed to differences in muscular performance among mutants was addressed by examining worms in which expression of wild-type body-wall isoforms was blocked by RNA interference (RNAi; Fire et al., 1998). Combined interference of F42E11.4 and T20B3.2 did not prove useful. A fraction, varying from one trial to another, of doubly treated mutants died prior to adulthood, and those that attained adulthood frequently displayed detachment of the hypodermis from the cuticle, as well as a very sickly, scrawny

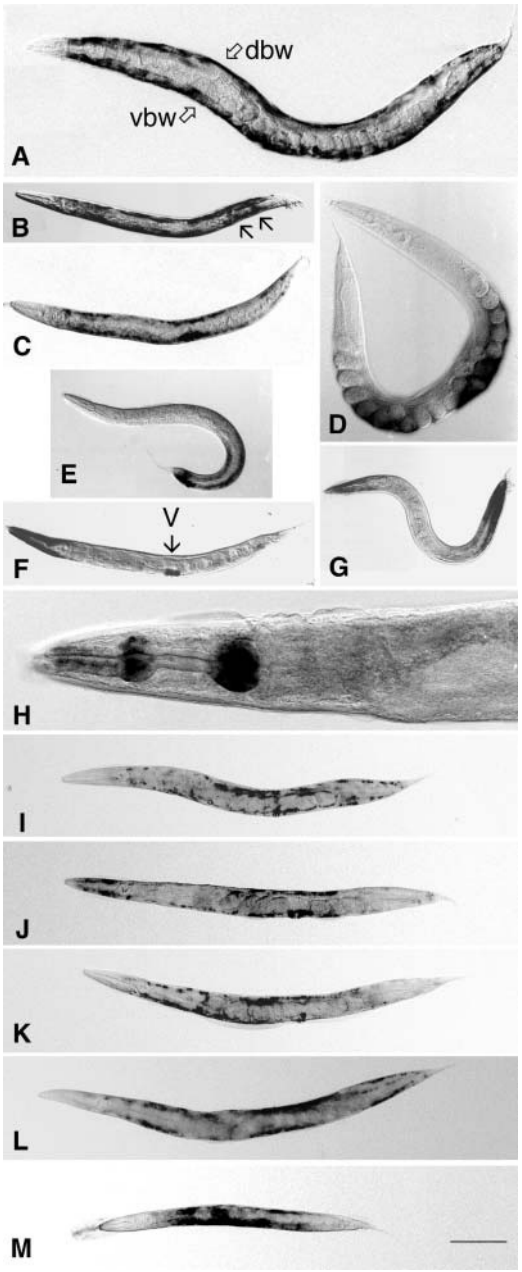

FIGURE 4 Localization of TnI mRNA in wild-type larvae and adults (*A–H*), TnI mRNA in *unc-27* mutants (*I* and *J*), and TnT and TnC mRNA in mutants (*K–M*). Transcripts of ZK721.2/*unc-27* were detected in the body-wall musculature of larvae and adults, as signaled by the darkly stained cells running from head (oriented to left of panel) to tail. Unfilled arrows in *A* identify dorsal, dbw, and ventral, vbw, quadrants of body-wall muscle in an adult hermaphrodite. Filled arrows in *B* mark in an adult male expression in the diagonal sex muscles (the dorsoventral staining apparent at posterior of male in *B*), complementing expression in the male's body-wall muscle. F42E11.4 transcripts were detected in body-wall musculature of larvae, as well as in the proximal gonad of both sexes (*C*, fourth larval stage, or L4, hermaphrodite; *D*, adult hermaphrodite, showing staining of the uteri, in which eggs are visible; and *E*, L4 male). T20B3.2 transcripts localized to anteriormost body-wall muscle cells and vulval muscles (marked *V*) of hermaphrodites (*F*). In males, T20B3.2 transcripts were detected in anteriormost and posterior body-wall muscle cells, as well as sex-specific muscles at the tail (*G*). In both sexes, W03F8.1 transcripts were detected throughout the pharyngeal musculature (*H*). Expression patterns of troponin isoforms in *unc-27* mutants are illustrated with *su142*sd worms in panels *I-M*. Transcripts of TnI isoforms F42E11.4 (*I*) and T20B3.2 (*J*) were detected in body-wall muscle of a fraction of adult mutant hermaphrodites. Expression of body-wall isoforms of TnT (*mup-2*/T22E5.5 in *K* and F53A9.10 in *L*) and TnC (*pat-10*/F54C1.7 in *M*) in the mutants resembled the wild-type patterns, with the exception that transcripts of the major embryonic body-wall TnT (*mup-2*) remained detectable in body-wall muscle of some mutant adults. Scale, 15 μm for panel *H* and 50 μm for others.

appearance suggestive of starvation, likely arising from inability of the worms to move their heads to obtain food.

Following interference of F42E11.4, a high percentage of *su142*sd and *e155* animals became completely immobile (e.g., 100% immobility in two of four trials; these worms still could move their heads to forage, presumably because of expression of T20B3.2 in the anteriormost body-wall muscle cells). Wild types and, to a lesser extent, *su195*sd worms subjected to RNAi of F42E11.4 remained mobile. Wave frequency was 1.48 $\pm$ 0.27 Hz ($n = 12$) for wild-type (compare with 1.56 $\pm$ 0.19 Hz, $n = 12$, for ''negative control'' wild-types soaked in buffer lacking dsRNA; $P > 0.40$ by nondirectional t-test) and 0.28 $\pm$ 0.14 Hz ($n = 10$) for the mutant. The degree of rigid paralysis within the mutants was consequently gauged from dimensions of the worms, because hypercontracted worms have previously been shown to take on a ''dumpy'' appearance, due to diminution of both the body length and the length/width ratio (Reiner et al., 1995). Results following interference of F42E11.4 are given in Table 2, with column two (labeled immobile subset) giving mean length of worms from the two trials in which complete immobility was displayed by *su142*sd and *e155* worms, and with column three summarizing results pooled from all four trials. In both the subset and the pooled data, treated *su142*sd worms were shorter than the *e155* ones (for the subset data $P = 0.011$ with Tukey's honestly significant difference test and 0.004 with the Games-Howell test; for the pooled data, $P \ll 0.001$ with both tests). Although exhibiting some ability to move, the *su195*sd worms also were short, with a length indistinguishable from that of *su142*sd worms ($P > 0.15$ in both cases).

The relative extents of compensation by F42E11.4 and T20B3.2 for mutant ZK721.2 was addressed with *e155* worms, because working with these avoided complications of semidominance. Length of adults following RNAi of F42E11.4 was 0.62 $\pm$ 0.15 mm (mean $\pm$ SD, $n = 47$ worms), but for those subjected to RNAi of T20B3.2 length was 0.77 $\pm$ 0.10 mm ($n = 18$) (comparison of the two means gives $P < 0.001$). Note that *e155* worms subjected to a control RNAi procedure, having an incubation in 0 μg/μl RNA, had a mean adult length of 0.88 $\pm$ 0.11 mm ($n = 23$). Thus, the impact on mean adult length following depletion of T23B3.2 is about one-third of that following depletion of F42E11.4.

TABLE 1 Frequency of contractile waves passing along body wall of swimming worms

	Homozygous first-stage larvae, Hz	Homozygous third-stage larvae, Hz	Homozygous adults, Hz	Heterozygous adults (+/−), Hz
Wild-type	1.72 ± 0.14 (10)	1.83 ± 0.17 (12)	1.84 ± 0.09 (12)	
*su142*sd	0.92 ± 0.29 (10)	0.12 ± 0.10 (12)	0.21 ± 0.14 (15)	1.53 ± 0.19 (16)
e155	1.22 ± 0.21 (10)	0.82 ± 0.24 (12)	0.60 ± 0.16 (15)	1.82 ± 0.15 (19)
*su195*sd	1.39 ± 0.29 (15)	0.54 ± 0.14 (15)	0.24 ± 0.08 (15)	1.58 ± 0.24 (16)

Values are mean ± SD, with number of worms analyzed in parentheses. Temperature was 23–25°C. For each of the three columns pertaining to homozygotes, as well as for the heterozygotes compared with wild-type homozygotes, the global null hypothesis of equality among means was rejected ($P < 0.001$; ANOVA F test). Post hoc comparisons within data for adult homozygotes led to rejection of null hypothesis ($P < 0.001$; Tukey's honestly significant difference test) for each pair except *su142*sd versus *su195*sd ($P > 0.9$). For adult heterozygous mutants and wild-type adults, post hoc comparisons led to rejection of null hypothesis ($P < 0.005$) for each pair except *su142*sd versus *su195*sd and *e155* versus wild-type ($P > 0.8$).

Structure of *unc-27* mutant muscle

Structural analyses were undertaken to gain insight on the mechanism by which the mutations compromise muscular activity. Both polarized light microscopy with living worms and antivinculin labeling of fixed worms revealed a distortion of sarcomeric organization in the body-wall muscle of the mutants (Fig. 6). The wild-type pattern of obliquely arranged, alternating isotropic and anisotropic bands that is seen in wild-type worms (Fig. 6 *B*) was absent in mutants (exemplified with *su142*sd, shown in Fig. 6 *D*). Dense bodies, marking the ends of the sarcomeres and equivalent to Z-lines, were evenly spaced along parallel rows in wild-type worms, as indicated by the position of vinculin foci (Fig. 6 *A*), but their disposition was greatly distorted in the mutants (Fig. 6 *C*).

Electron microscopy of body-wall muscle confirmed a prevalent disorder of dense body positioning and a less well-defined sarcomeric structure. In longitudinal sections (Fig. 7), it is clear that the oblique striation is disarrayed, so that the positioning of the dense bodies (equivalent to Z-lines) is not as regular. The reason for this appearance was identified from transverse sections. In wild-type worms (Fig. 8, *A* and *B*), well-oriented cross sections showed sharp profiles of thin and thick filaments and a regular alternation of the sarcomere bands. Within half-sarcomeres, dense bodies were followed by I bands, composed of thin filaments, then by overlap zones of A bands, with regularly packed thick filaments surrounded by rings of thin filaments, and finally by the H zone of A bands, containing only thick filaments. The boundaries between the various bands were fairly abrupt and regular. With the mutants, the same bands were seen, but their positioning was irregular. The defects appeared strongest in the *su142*sd mutants (Fig. 8, *C–F*), but they were also clearly evident in the other two (Fig. 9). Small islands of thin filaments were interspersed within the overlap region of A bands and even within the H zone. In the overlap region, the content of thin filaments was quite variable, and the H zone was fragmented into several small areas of the cross section. The Z-lines had irregular boundaries. The images do not suggest any basic defect in the formation of filaments or in their assembly into the basic components of a sarcomere. The structural disruption evidenced by the mutants' muscle could arise from unregulated contraction of the sarcomere, in which small portions of each myofibril shorten irregularly and independently from one another, thereby distorting the filament disposition (Fig. 7 *D*).

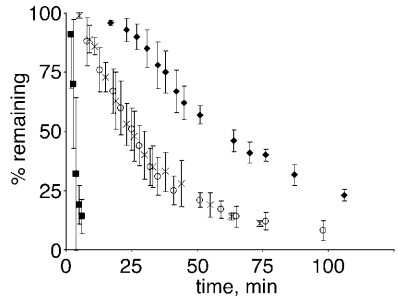

FIGURE 5 Chemotaxis assay with wild-type (*solid squares*), *su142*sd (*solid diamonds*), *e155* (*open circles*), and *su195*sd (*crosses*) adults. The percentage of worms remaining within the annular ring of bacteria is plotted as a function of time, in minutes. Data are means from seven trials with wild-types and from four trials with each mutant strain; bars give ±1 standard deviation. In the assay, $t_{1/2} = 3.29 \pm 0.48$ min for wild-type, 24.35 ± 4.56 min for *e155*, 25.07 ± 5.62 min for *su195*sd, and 59.72 ± 5.17 min for *su142*sd. The global null hypothesis of equality among half-times was rejected ($P < 0.001$; ANOVA F-test). Post hoc comparisons led to rejection of null hypothesis for the following: 1), wild-type versus each mutant ($P < 0.001$; Tukey's honestly significant difference test); and 2), *su142*sd versus *e155* and *su195*sd ($P < 0.001$).

DISCUSSION

When expressed in vivo, all three truncation mutants of TnI lead to disarray of the sarcomere and rigid paralysis. Three observations suggest that this phenotype is a primary consequence of the mutations, as opposed to a secondary complication resulting, for example, from alterations of relative protein levels. First, the semidominance of *su142*sd and *su195*sd, given the absence of haploinsufficiency, indicates that mutant TnI protein is indeed synthesized and able to compete with wild-type TnI. Second, although associated with the mutations, changes in the expression pattern of troponin subunits appeared limited, affecting a minority of examined worms and involving persistence of

TABLE 2 Adult body length of worms subjected to RNAi of F42E11.4 TnI

	Untreated control, mm	Immobile subset, mm	Pooled data, mm
Wild-type	1.19 ± 0.05 (12)	1.09 ± 0.13 (22)	1.04 ± 0.13 (58)
*su142*sd	0.96 ± 0.05 (14)	0.47 ± 0.06 (38)	0.47 ± 0.07 (69)
e155	1.03 ± 0.08 (20)	0.56 ± 0.11 (29)	0.62 ± 0.15 (47)
*su195*sd	1.00 ± 0.07 (20)	0.50 ± 0.12 (49)	0.50 ± 0.12 (101)

Values are mean ± SD, with number of adults analyzed in parentheses. For each of the three columnar groupings, the global null hypothesis of equality among means was rejected ($P < 0.001$; ANOVA F test). Post hoc comparisons within columns led to rejection of null hypothesis for the following: 1), wild-type versus each mutant ($P < 0.001$; Tukey's honestly significant difference test) for the three columns; 2), *su142*sd versus *e155* for immobile ($P = 0.011$) and pooled ($P < 0.001$) cases; and 3), *e155* versus *su195*sd for the pooled case ($P < 0.001$). For the untreated case, comparison of *su142*sd with *e155* was suggestive of a difference ($P = 0.024$). In a negative control involving treatment of worms with 0 μg/μl RNA, mean length was 1.10 ± 0.08 mm (10) for wild-types, and it was 0.88 ± 0.11 (23) for *e155*.

embryonic-larval isoforms in adult muscle, as well as in the case of TnI T20B3.2 an increase in number of cells showing expression. Third, the structure of mutant muscle is entirely consistent with disarrangement of the sarcomeres, rather than with defects typically associated with altered protein levels such as improperly formed filaments and failed assembly of basic components of the sarcomere. Thus, in the subsequent discussion, the phenotype is interpreted in light of both the structure of crystalline human cardiac troponin (Takeda et al., 2003) and the substantial body of biochemical work with TnI in vitro (comprehensively reviewed by Perry, 1999).

Paralysis caused by *e155*

Adult *e155* animals showed a surprising degree of swimming and crawling capability, contrary to predictions based on previous work with vertebrate troponins. Biochemical studies show that in the absence of TnI vertebrate thin filaments are disinhibited (reviewed by Perry, 1999). Extending this finding, extraction of TnI from permeabilized ventricular muscle leads to calcium-independent tension (Strauss et al., 1992), and myocardium from mice in which the cardiac TnI gene had been deleted exhibited abnormally shortened sarcomeres and elevated resting tension (Huang et al., 1999). The *e155* mutation eliminates all but 9 of the 242 residues of ZK721.2, including all of the hallmarks of TnI, and therefore it is unlikely that the truncated protein could fulfill any roles of wild-type TnI. One possible explanation for the residual locomotion of *e155* animals is redundancy within the activation process due to potential presence of thick- and thin-filament regulation, whereas another is overlapping expression of TnI isoforms.

Dual-regulation is prevalent throughout the animal kingdom (Lehman and Szent-Gyorgyi, 1975), and early evidence suggested existence in *C. elegans* of thick-filament-based regulation or modulation (Harris et al., 1977). Little is known about the specific roles of thick- and thin-filament regulatory proteins in dually regulated muscle, but available data, from studies with *Limulus* muscle, suggest that both regulatory systems need to be switched on before activation of actomyosin MgATPase and tension development can occur (Wang et al., 1993). If dually regulated in the same manner as *Limulus* muscle, *C. elegans* body-wall muscle depleted of TnI should be capable of contracting and relaxing: thin filaments would be persistently disinhibited, and the thick-filament-based system would toggle on and off. The complete immobility of *e155* worms depleted of the embryonic-larval TnI (F42E11.4) conflicts with this prediction and suggests that body-wall muscle is regulated solely by troponin, a possibility which does not exclude thick-filament-based modulation by a protein such as twitchin/UNC-22 (Benian et al., 1989). Additionally, the loss of mobility, as well as diminution of body length, of *e155* worms subjected to RNAi offers clear evidence that the

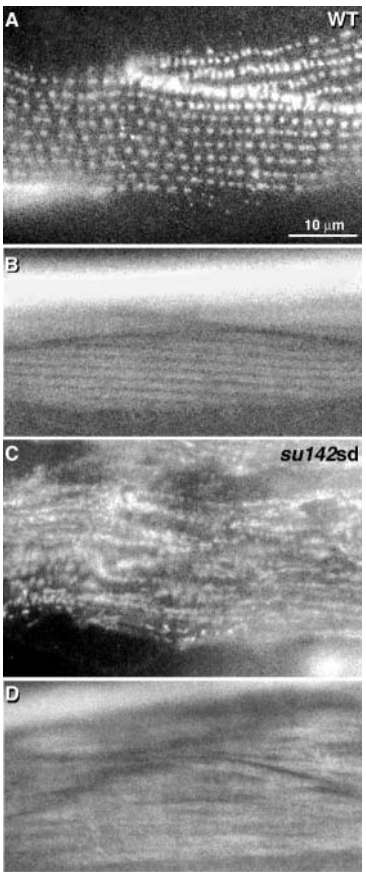

FIGURE 6 Structure of wild-type and *unc-27* mutant body-wall muscle revealed by reaction of adults with antivinculin antibody (*A* and *C*) and by visualization of living worms between crossed polarizers (*B* and *D*). The wild-type muscle (*A* and *B*) shows obliquely arranged, alternating isotropic and anisotropic bands, as well as evenly spaced rows of dense bodies, labeled by antivinculin. In the mutants, exemplified by *su142*sd (*C* and *D*), the pattern of alternating bands was absent, and the disposition of dense bodies was greatly distorted.

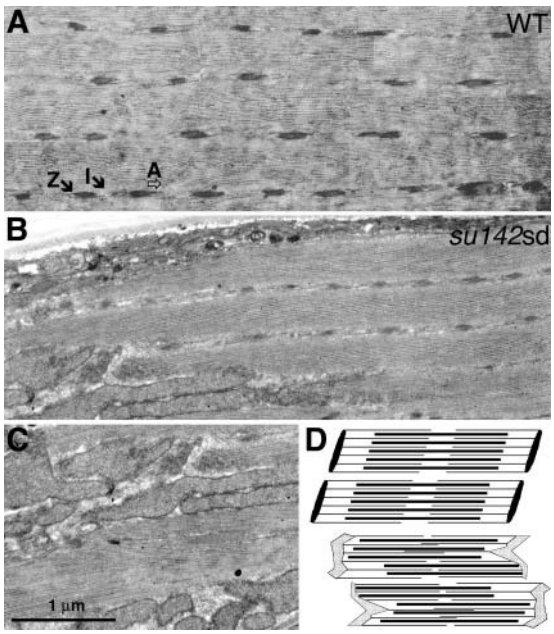

FIGURE 7 Longitudinal sections through wild-type (*A*) and *su142*sd (*B* and *C*) muscle fibers. In *A*, the vinculin containing dense bodies are located at periodic intervals and are well aligned. Note short, well delineated vinculin-containing dense bodies (equivalent to Z-lines) flanked by short, pale I bands, followed by the A bands that occupy most of the sarcomere. These three regions are identified for one half-sarcomere; note that the sarcomere-length is ~12 μm and that the bands are oriented ~6° with respect to the filaments' long axis, rather than 90° as seen in cross-striated muscle. (*B*) A rare region in the mutant muscle that maintains a fairly well-ordered striation and is seen in the same orientation as in *A*. However, in the lower right corner of *B*, the striation is lost, and a less well-ordered arrangement of sarcomere bands prevails. (*C*) A continuation of the image in *B*, along the same fiber (notice the same mitochondria on the left). In this area the striation is not visible, the Z-lines are irregular in aspect and occurrence, and I bands are not detectable. (*D*) A cartoon contrasting wild-type (*upper two images*) and mutant (*lower two images*) sarcomeres.

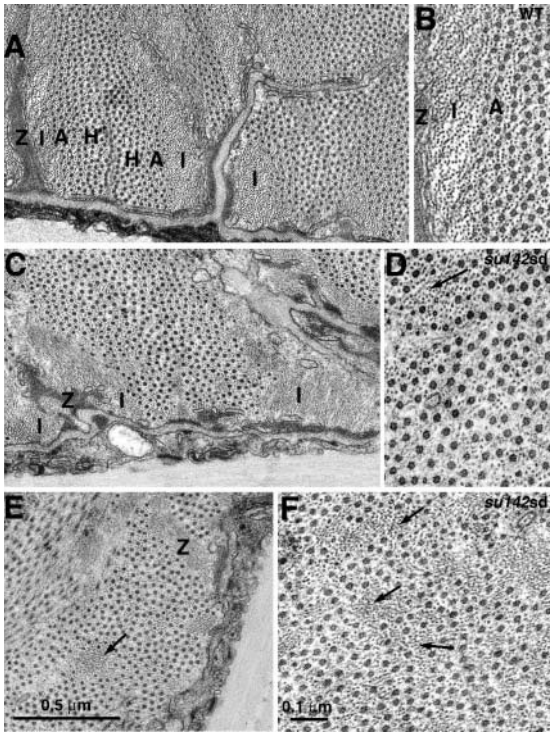

FIGURE 8 Comparison of cross sections through muscle fibers of wild-type (*A* and *B*) and *su142*sd mutant (*C–F*) worms. In the wild-type (*A* and *B*), orderly arrangement of thin and thick filaments within ''obliquely striated'' sarcomeres is indicated by the orderly banding pattern as the section cuts through Z-lines (*Z*), I bands (*I*), overlap regions of A bands (*A*), and H zones (*H*). Each of the bands occupies a strip of the image, and the borders between the different regions are well delimited. The thick filaments taper in an orderly manner on either side of the A band, and the transition between the I and A bands is fairly sharp, indicating that thick filaments are approximately of the same length and are aligned with each other. At higher magnification (*B*), regular rings of thin filaments surround each thin filament. In the mutant (*C–F*), several structural features indicate that the sarcomere is seriously disarranged. The dense areas representing dense bodies or Z-lines (*Z*) have variable, rough outlines; groups of thin filaments (*arrowheads*) are not limited to the I bands but are seen in the middle of the A bands, between groups of thick filaments. There are no orderly borders between I and A bands, and the H zone is also dispersed over various portions of the cross section. Various numbers of thin filaments (from none to a double ring) surround each thick filament. This appearance results from loss of the lateral alignment of the filaments, with groups of them slipping off toward one end or the other of the sarcomere and irregularly pulling on the Z-lines.

embryonic-larval isoform can compensate for loss of the larval-adult isoform (ZK721.2/*unc-27*) and account for regulated contraction in body-wall muscle of *e155* animals.

Paralysis caused by *su142*sd

An interesting question arising from the data is why *su142*sd, which eliminates the inhibitory region of TnI, is more deleterious than *e155*, a presumed null. The disparity likely reflects differing extents of compensation for the two alleles by other TnI isoforms, as well as true difference in effects of the mutant alleles. At a qualitative level, both mutations are associated with comparable alterations of the expression pattern of troponin isoforms, e.g., persistence of embryonic-larval TnI (F42E11.4) and TnT (*mup-2*/*tnt-1*/T22E5.5) transcripts in body-wall muscle in a minority of adults. Yet, the semidominance of *su142*sd, in the absence of haploinsufficiency, indicates that this mutant TnI can compete with wild-type TnI and hence that compensation by wild-type TnI should be less in *su142*sd animals than in *e155* ones.

Although fully supportive of differing extents of compensation for *su142*sd and *e155*, the data are also compatible with a true difference between effects of the mutations. When depleted of the embryonic-larval body-wall TnI (F42E11.4), the *su142*sd worms were shorter than the *e155* ones, an observation compatible with a greater degree of hypercontraction in the former. It remains possible that RNAi did not remove all traces of compensation by F42E11.4; however, the complete immobility of both *e155* and *su142*sd worms following RNAi of F42E11.4 suggests

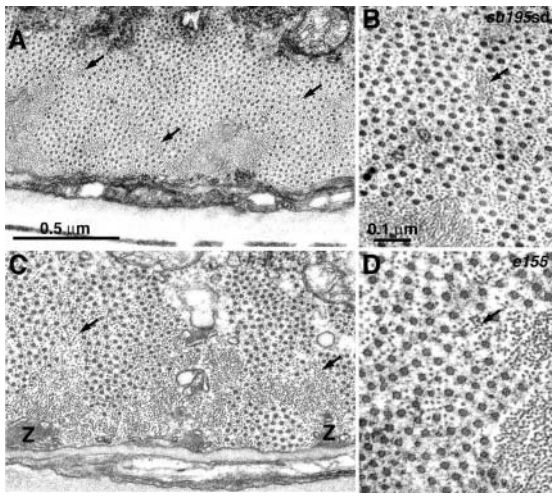

FIGURE 9 Cross sections through muscle fibers of the *su195*sd mutant (*A* and *B*) and the *e155* mutant (*C* and *D*). The sharp, round profiles of thin and thick filaments indicate that the sections are well oriented in a direction perpendicular to the long axis of the fiber. Despite the good orientation of the section, the appearance of the sarcomere bands and the disposition of the filaments are disorderly, indicating a basic lack of alignment in both mutants. The presence of large groups of thin filaments in the A band (*arrowheads*) indicates that groups of thick filaments have pulled away to one side of the sarcomere. Variability in the ratio of thin to thick filaments in immediately adjacent areas throughout the A band is also indicative of a disordered alignment, probably due to the sliding of individual filaments toward one or the other Z-line. Z-line profiles (*Z*) are fragmented, indicating that the Z-lines have an uneven profile.

at the functional level absence of significant compensation. This immobility likewise argues against meaningful compensation afforded by T20B3.2, transcripts of which were detected in the middle and posterior body-wall muscle of a minority of adult mutants.

Thus, the fragment encoded by *su142*sd, terminating at a position equivalent to Lys^{87} of rabbit fast TnI and Lys^{120} of human cardiac TnI, both competes with wild-type TnI and likely wreaks more damage than does the absence of TnI. The fragment's ability to compete in vivo agrees well with the structure of crystalline human cardiac troponin, in which TnI residues 42–136 associate with TnT residues 203–271 and TnC residues 93–161 to form the IT-arm (Takeda et al., 2003). Biochemical work substantiates an interaction in vitro between vertebrate TnT and the N-terminal half of TnI (Farah et al., 1994; Van Eyk et al., 1997).

The greater severity of the *su142*sd mutation in comparison with the null following RNAi may reflect participation of the N-terminal half of TnI in activation, i.e., the enhancement of actomyosin MgATPase in the presence of activating calcium to an activity exceeding that observed with actin-tropomyosin-myosin in vitro (Malnic et al., 1998). In this sense, a parallel may be drawn between the severity of *su142*sd and the muscle degeneration caused by the *Drosophila* TnI $heldup^2$ mutation, which replaces with valine an invariant alanine falling within the IT-arm and aligning with rabbit fast residue 25 and human cardiac residue 57 (Beall and Fyrberg, 1991). The degeneration can be ameliorated by elimination of myosin filaments, as well as by other myosin mutations, suggesting that $heldup^2$ promotes excessive actin-myosin interaction and force production (Beall and Fyrberg, 1991; Kronert et al., 1999).

Paralysis caused by *su195*sd

The most striking aspect of sarcomeric disarray and paralysis caused by *su195*sd is the extent to which the phenotype resembles that of the presumed null, *e155*, even though the *su195*sd mutation leaves intact all but the extreme C-terminus. Loss of TnI function caused by *su195*sd could suggest that the mutant protein simply fails to associate with the thin filament, but both the semidominance of the mutation and the mobility of *su195*sd worms subjected to RNAi of F42E11.4 argue against this view. Another possibility is that the extreme C-terminus is needed for the full inhibitory potential of TnI to be manifested. This view is supported by work with vertebrate TnI, even though the extreme C-termini of vertebrate and invertebrate isoforms differ in length and composition. For example, removal of the C-terminal 17 residues from cardiac TnI leads to diminished calcium sensitivity of force, and removal of 23 residues leads to increased sensitivity, as well as impaired ability of the truncated TnI to inhibit (Rarick et al., 1997). Elimination of as few as 18 residues from the C-terminus of chicken fast skeletal TnI compromises inhibition of actomyosin MgATPase (Ramos, 1999).

Biological relevance of the extreme C-terminus of TnI is reflected in several observations. Four missense mutations and an eight-residue deletion near the C-terminus of human cardiac TnI have been linked to cardiomyopathy (Kimura et al., 1997; Morner et al., 2000; Morgensen et al., 2003). Cleavage of the C-terminal 17 residues from cardiac TnI ensues ischemia and reperfusion injury (McDonough et al., 1999), and the steady-state force-calcium relation obtained with myocardium regulated by the truncated TnI exhibits both diminished peak force and depressed calcium sensitivity (Murphy et al., 2000). The ability of the C-terminus to modulate TnI's inhibitory strength potentially is tapped in nature. Encoding the C-terminus of *Drosophila* TnI are two exons (exons 9 and 10) that are spliced in a mutually exclusive manner (Barbas et al., 1991). The sequence encoded by exon 9 is detected only in adult isoforms and differs in two obvious respects from that of exon 10. The terminus generated by exon 9 is shorter by nine residues, and it lacks a motif (P/G–D/E–W–R/S–K) found in almost all other TnI isoforms of invertebrates and vertebrates, with notable exceptions being *C. elegans* isoform W03F8.1, expressed exclusively in the pharynx, and TnI of crayfish and scallop.

In summary, the rigid paralysis and sarcomeric disarray of the three mutants are consistent with unregulated contraction

of the mutant sarcomeres, in which small portions of each myofibril shorten irregularly and independently from one another, thereby distorting the filament disposition. Semidominance of two of the alleles, in the absence of haploinsufficiency, highlights that mutant protein is synthesized and competes with wild-type isoforms. The exacerbated deficits exhibited by *su142*sd (Gln^{122}stop) mutants strengthen the view that in vivo the N-terminal portion of TnI enhances force production. The deleterious effects of the *su195*sd (Glu^{207}stop) allele point strongly to a role of the extreme C-terminus in TnI's inhibitory function.

We thank Drs. S. Takeda and Y. Maéda for kindly providing a preprint of their article on crystalline troponin.

We gratefully acknowledge funding from National Institutes of Health grant 5-PO1-HL15835 to the Pennsylvania Muscle Institute (C.F.-A.), as well as from the Templeton Medical Research Foundation and the National Science Foundation (IBN 9985315) (T.A.). Nematode strains used in this work were provided by the *Caenorhabditis* Genetics Center, which is funded by the National Center for Research Resources of the National Institutes of Health.

REFERENCES

Allen, T. StC., K. McArdle, E. Polyak, and E. A. Bucher. 1997. Troponin T diversity and function in *C. elegans*. *Biophys. J.* 72:58a. (Abstr.)

Altschul, S. F., W. Gish, W. Miller, E. W. Myers, and D. J. Lipman. 1990. Basic local alignment search tool. *J. Mol. Biol.* 215:403–410.

Barbas, J. A., J. Galceran, I. Krah-Jentgens, J. L. de la Pompa, I. Canal, O. Pongs, and A. Ferrus. 1991. Troponin I is encoded in the haplolethal region of the Shaker gene complex of *Drosophila*. *Genes Dev.* 5:132–140.

Beall, C. J., and E. Fyrberg. 1991. Muscle abnormalities in *Drosophila melanogaster heldup* mutants are caused by missing or aberrant troponin-I isoforms. *J. Cell Biol.* 114:941–951.

Benian, G. M., J. E. Kiff, N. Neckelmann, D. G. Moerman, and R. H. Waterston. 1989. Sequence of an unusually large protein implicated in regulation of myosin activity in *C. elegans*. *Nature*. 342:45–50.

Brenner, S. 1974. The genetics of *Caenorhabditis elegans*. *Genetics.* 77:71–94.

Epstein, H. F., M. M. Isachsen, and E. A. Suddelson. 1976. Kinetics of movement of normal and mutant nematodes. *J. Comp. Physiol. [A].* 110:317–322.

Farah, C. S., C. A. Miyamoto, C. H. I. Ramos, A. C. R. da Silva, R. B. Quaggio, K. Fujimori, L. B. Smillie, and F. C. Reinach. 1994. Structural and regulatory functions of the NH_2- and COOH-terminal regions of skeletal muscle troponin I. *J. Biol. Chem.* 269:5230–5240.

Finney, M., and G. B. Ruvkin. 1990. The *unc-86* gene product couples cell lineage and cell identity in *C. elegans*. *Cell.* 63:895–905.

Fire, A., S. Xu, M. K. Montgomery, S. A. Kostas, S. E. Driver, and C. C. Mello. 1998. Potent and specific genetic interference by double-stranded RNA in *Caenorhabditis elegans*. *Nature.* 391:806–811.

Greenstein, D., S. Hird, R. H. Plasterk, Y. Andachi, Y. Kohara, B. Wang, M. Finney, and G. Ruvkin. 1994. Targeted mutations in the *Caenorhabditis elegans* POU homeo box gene *ceh-18* cause defects in oocyte cell cycle arrest, gonad migration, and epidermal differentiation. *Genes Dev.* 8:1935–1948.

Harris, H. E., M.-Y. Tso, and H. F. Epstein. 1977. Actin and myosin-linked calcium regulation in the nematode Caenorhabditis elegans. Biochemical and structural properties of native filaments and purified proteins. *Biochemistry.* 16:859–865.

Henikoff, S., J. G. Henikoff, W. J. Alford, and S. Pietrokovski. 1995. Automated construction and graphical presentation of protein blocks from unaligned sequences. *Gene.* 163:GC17–GC26.

Hill, A. V. 1927. Living Machinery. Harcourt, Brace and Co., New York.

Huang, X., Y. Pi, K. J. Lee, A. S. Henkel, R. G. Gregg, P. A. Powers, and J. W. Walker. 1999. Cardiac troponin I gene knockout. *Circ. Res.* 84:1–8.

Kimura, A., H. Harada, J. Park, H. Nishi, M. Satoh, M. Takahashi, S. Hiroi, T. Sasaoka, N. Ohbuchi, T. Nakamura, T. Koyanagi, T.-H. Hwang, J.-A. Choo, K.-S. Chung, A. Hasegawa, R. Nagai, O. Okazaki, H. Nakamura, M. Matsuzaki, T. Sakamoto, H. Toshima, Y. Koga, T. Imaizumi, and T. Sasazuki. 1997. Mutations in the cardiac troponin I gene associated with hypertrophic cardiomyopathy. *Nat. Genet.* 16:379–382.

Kolmerer, B., J. Clayton, V. Benes, T. Allen, C. Ferguson, K. Leonard, U. Weber, M. Knekt, W. Ansorge, S. Labeit, and B. Bullard. 2000. Sequence and expression of the kettin gene in *Drosophila melanogaster* and *Caenorhabditis elegans*. *J. Mol. Biol.* 296:435–448.

Kronert, W. A., A. Acebes, A. Ferrús, and S. I. Bernstein. 1999. Specific myosin heavy chain mutations suppress troponin I defects in *Drosophila* muscles. *J. Cell Biol.* 144:989–1000.

Lehman, W., and A. G. Szent-Gyorgyi. 1975. Regulation of muscle contraction. Distribution of actin control and myosin control in the animal kingdom. *J. Gen. Physiol.* 66:1–30.

Maeda, I., Y. Kohara, M. Yamamoto, and A. Sugimoto. 2001. Large-scale analysis of gene function in *Caenorhabditis elegans* by high-throughput RNAi. *Curr. Biol.* 11:171–176.

Malnic, B., C. S. Farah, and F. C. Reinach. 1998. Regulatory properties of the NH_2- and COOH-terminal domains of troponin T. ATPase activation and binding to troponin I and troponin C. *J. Biol. Chem.* 273:10594–10601.

McDonough, J. L., D. K. Arrell, and J. E. Van Eyk. 1999. Troponin I degradation and covalent complex formation accompanies myocardial ischemia/reperfusion injury. *Circ. Res.* 84:9–20.

Miller, D. M., and D. C. Shakes. 1995. Immunofluorescence microscopy. *In Caenorhabditis elegans*: Modern Biological Analysis of an Organism. G. F. Epstein and D. C. Shakes, editors. Academic Press, San Diego, CA. 365–394.

Moerman, D., and A. Fire. 1997. Muscle: structure, function and development. *In C. elegans* II. D. Riddle, T. Blumenthal, and J. Priess, editors. Cold Spring Harbor Laboratory Press, New York. 417–470.

Morgensen, J., T. Kulbo, M. Duque, W. Uribe, A. Shaw, R. Murphy, J. R. Gimeno, P. Elliott, and W. J. McKenna. 2003. Idiopathic restrictive cardiomyopathy is part of the clinical expression of cardiac troponin I mutations. *J. Clin. Invest.* 111:209–216.

Morner, S., P. Richard, E. Kazzam, B. Hainque, K. Schwartz, and A. Waldenstrom. 2000. Deletion in the cardiac troponin I gene in a family from northern Sweden with hypertrophic cardiomyopathy. *J. Mol. Cell. Cardiol.* 32:521–525.

Murphy, A. M., H. Kogler, D. Georgakopoulos, J. L. McDonough, D. A. Kass, J. E. Van Eyk, and E. Marban. 2000. Transgenic mouse model of stunned myocardium. *Science.* 287:488–491.

Perry, S. V. 1999. Troponin I: inhibitor or facilitator. *Mol. Cell. Biochem.* 190:9–32.

Ramos, C. H. I. 1999. Mapping subdomains in the C-terminal region of troponin I involved in its binding to troponin C and to thin filament. *J. Biol. Chem.* 274:18189–18195.

Rarick, H. M., X.-H. Tu, R. J. Solaro, and A. F. Martin. 1997. The C terminus of cardiac troponin I is essential for full inhibitory activity and Ca^{2+} sensitivity of rat myofibrils. *J. Biol. Chem.* 272:26887–26892.

Reiner, D. J., D. Weinshenker, and J. H. Thomas. 1995. Analysis of dominant mutations affecting muscle excitation in *Caenorhabditis elegans*. *Genetics.* 141:961–976.

Sato, T. 1968. A modified method for lead staining of thin sections. *J. Electron Microsc.* 17:158–159.

Strauss, J. D., C. Zeugner, J. E. Van Eyk, C. Bletz, M. Troschka, and J. C. Ruegg. 1992. Troponin replacement in permeabilized cardiac muscle. *FEBS Lett.* 310:229–234.

Swofford, D. L. 2000. PAUP: Phylogenetic Analysis Using Parsimony and Other Methods. Sinauer Associates, Sunderland, MA.

Takeda, S., A. Yamashita, K. Maeda, and Y. Maéda. 2003. Structure of the core domain of human cardiac troponin in the Ca^{2+}-saturated form. *Nature*. 424:35–41.

Terami, H., B. D. Williams, S.-I. Kitamura, Y. Sakube, S. Matsumoto, S. Doi, T. Obinata, and H. Kagawa. 1999. Genomic organization, expression, and analysis of the troponin C gene *pat-10* of *Caenorhabditis elegans*. *J. Cell Biol.* 146:193–202.

Thompson, J. D., T. J. Gibson, F. Plewniak, F. Jeanmougin, and D. G. Higgins. 1997. The Clustal_X windows interface: flexible strategies for multiple sequence alignment aided by quality analysis tools. *Nucleic Acids Res.* 25:4876–4882.

Van Eyk, J. E., L. T. Thomas, B. Tripet, R. J. Wiesner, J. R. Pearlstone, C. S. Farah, F. C. Reinach, and R. S. Hodges. 1997. Distinct regions of troponin I regulate Ca^{2+}-dependent activation and Ca^{2+} sensitivity of the Acto-S1-TM ATPase activity of thin filament. *J. Biol. Chem.* 272:10529–10537.

Wang, F., B. M. Martin, and J. R. Sellers. 1993. Regulation of actomyosin interactions in *Limulus* muscle proteins. *J. Biol. Chem.* 268:3776–3780.

Williams, B. D., B. Schrank, C. Huynh, R. Shownkeen, and R. H. Waterston. 1992. A genetic mapping system in *Caenorhabditis elegans* based on polymorphic sequence-tagged sites. *Genetics*. 131:609–624.

Zengel, J. M., and H. F. Epstein. 1980. Identification of genetic elements associated with muscle structure in the nematode *Caenorhabditis elegans*. *Cell Motil.* 1:73–97.